Hindawi Publishing Corporation
Journal of Nanomaterials
Volume 2015, Article ID 276790, 7 pages
http://dx.doi.org/10.1155/2015/276790

Research Article

Study of Synchrotron Radiation Near-Edge X-Ray Absorption Fine-Structure of Amorphous Hydrogenated Carbon Films at Various Thicknesses

Sarayut Tunmee,[1] Ratchadaporn Supruangnet,[2] Hideki Nakajima,[2] XiaoLong Zhou,[1] Satoru Arakawa,[1] Tsuneo Suzuki,[3] Kazuhiro Kanda,[4] Haruhiko Ito,[1] Keiji Komatsu,[1] and Hidetoshi Saitoh[1]

[1]*Graduate School of Engineering, Nagaoka University of Technology, 16031-1 Kamitomioka, Nagaoka, Niigata 940-2188, Japan*
[2]*Synchrotron Light Research Institute (Public Organization), 111 University Avenue, Muang District, Nakhon Ratchasima 30000, Thailand*
[3]*Extreme Energy-Density Research Institute, Nagaoka University of Technology, 16031-1 Kamitomioka, Nagaoka, Niigata 940-2188, Japan*
[4]*Laboratory of Advanced Science and Technology for Industry, University of Hyogo, 3-1-2 Koto, Kamigori-cho, Ako-gun, Hyogo 678-1205, Japan*

Correspondence should be addressed to Sarayut Tunmee; s137011@stn.nagaokaut.ac.jp and Hidetoshi Saitoh; hts@nagaokaut.ac.jp

Received 9 September 2015; Revised 8 December 2015; Accepted 9 December 2015

Academic Editor: Hongbin Bei

The compositions and bonding states of the amorphous hydrogenated carbon films at various thicknesses were evaluated via near-edge X-ray absorption fine-structure (NEXAFS) and elastic recoil detection analysis combined with Rutherford backscattering spectrometry. The absolute carbon sp^2 contents were determined to decrease to 65% from 73%, while the hydrogen contents increase from 26 to 33 at.% as the film thickness increases. In addition, as the film thickness increases, the π^* (C=C), σ^* (C–H), σ^* (C=C), and σ^* (C≡C) bonding states were found to increase, whereas the π^* (C≡C) and σ^* (C–C) bonding states were observed to decrease in the NEXAFS spectra. Consequently, the film thickness is a key factor to evaluate the composition and bonding state of the films.

1. Introduction

Amorphous hydrogenated carbon (*a*-C:H) films have attracted considerable attention in recent years for many reasons, such as excellent corrosion resistance, high hardness, high wear resistance, and good biocompatibility [1, 2]. Therefore, these films have the potential for many applications, for example, magnetic storage disks, automotive industry, biomedical parts, and solar cells [1–3]. The structure of *a*-C:H films is complex, being comprised of an amorphous mixture of sp^2 and sp^3 hybridized carbon atoms combined with hydrogen atoms in the local structure [4]. The chemical structure in terms of the coordination of carbon (sp^2 and sp^3 hybridization) and hydrogen atoms is one of the most important factors governing the quality of *a*-C:H films. The chemical structure of these films can be extracted using various conventional methods, such as Raman spectroscopy, Auger electron spectroscopy, and electron energy-loss spectroscopy [5]. However, in the last decade, powerful techniques, such as near-edge X-ray absorption fine-structure (NEXAFS) spectroscopy and photoelectron spectroscopy (PES), have been combined with the use of synchrotron radiation (SR) to study the chemical characteristics of films [6, 7]. Previous works [4, 6–8] have reported that both NEXAFS and PES can successfully extract the chemical structures of diamond-like carbon (DLC) films. SR is a source of electromagnetic waves that has several distinctive advantages over conventional sources, including broad spectrum, high brightness, high degree of collimation, well-defined polarization, and pulsed time structure [9]. Therefore, the SR source is one of the best sources for characterizing the local structures of films.

Because NEXAFS spectroscopy probes a nanometer-scale depth, the structural information gained by this analytical method may differ from the outcomes of analyses performed using techniques that provide different information in the depth direction [10]. NEXAFS spectroscopy is sensitive to the coordination of carbon atoms because it probes the absorption of SR by excitation of core electrons into unoccupied states. This probe exhibits strong and striking features of the absorption edge (e.g., *K*-edge), enabling the identification of the bonding configurations and hybridization states of carbon atoms in the near-surface region [9–12]. For *a*-C:H films, the spectrum has been decomposed into the main two-edge structure originating from π^* and σ^* orbitals, and the bonding configuration structure has been studied in detail [13, 14]. This spectroscopy has been established as an efficient method to quantify the sp^2 content of the film [15–17]. However, only a small number of studies have been performed to date [11, 15] on the compositions and bonding states; such studies provide deep insight into the evaluation of *a*-C:H films at various thicknesses.

In a previous study by Buijnsters et al. [4], the stability of hydrogen atoms in *a*-C:H films indicated that these atoms were terminated within the carbon matrix. To date, the relationship between the atomic compositions of hydrogen and carbon in these films has primarily been investigated using the combination of elastic recoil detection analysis (ERDA) and Rutherford backscattering spectrometry (RBS) with 2.5 MeV-He^+ irradiation, which is optimal for estimating the relative hydrogen content [18]. By analyzing the data from both methods, it is possible that nearly isolated hydrogen atoms exist in the films.

The relationship between film thickness and the true density of the film is important for characterizing the compositions and bonding states of films. According to recently reported papers [21, 22], the film thickness plays an important role in the formation not only of the surface characteristics but also of the feature of the π^* peak of the NEXAFS spectra. It has been interpreted that the atomic compositions of the film depended on the variation of the thickness. Thus, the film thickness is an attractive parameter to examine in conjunction with the compositions and the bonding states. For measuring the film thickness, the X-ray reflectivity (XRR) is a powerful technique due to its nondestructive nature for determining the layer thickness and true density of films.

The aim of this study is to investigate the chemical characteristics of films, particularly the compositions and bonding states at various thicknesses using NEXAFS spectroscopy at the 3.2a beamline at the synchrotron facility in Thailand. In addition, hydrogen content analysis is performed using the combination of ERDA and RBS in this work.

2. Experimental

First, the *p*-type silicon (Si) substrates were prepared into samples of 1 cm × 1 cm × 0.1 cm in size. All of the substrates were gently washed in the ultrasonic batch filled with the acetone and ethanol solutions each for 45 min. Before undertaking the film deposition process, the Si substrate surfaces were sputtered by argon ions at −0.3 kV of bias voltage to remove the native oxides formed on the substrate surface. Next, the *a*-C:H films were deposited onto the Si substrates via a radio-frequency plasma-enhanced chemical vapor deposition (RF-PECVD, 13.56 MHz) method with −0.4 kV of bias voltage under a working pressure of ~26.6 Pa. The films were fabricated from 25 cm^3/min benzene (99.99%), 15 cm^3/min hydrogen gas (99.999%), and 15 cm^3/min argon gas (99.9999%), with their flows being controlled by mass flow controllers (MFCs).

The thickness and true density of the *a*-C:H films were measured using XRR equipped with a Cu-Kα radiation source emitting at a wavelength of 1.541 Å. The XRR profiles of the films were simulated by using GXRR software, which is the commercial package of analysis based on Parratt's method [23].

The NEXAFS measurement was performed at the end-station of the 3.2a beamline in the Synchrotron Light Research Institute (Public Organization), Nakhon Ratchasima, Thailand. The beamline photon source covers an energy range of 40 to 1040 eV at the resolving power of 10,000. The SR source at the storage ring was generated using a beam energy of 1.2 GeV; the details of this beamline's specifications and performance were reported elsewhere [24, 25]. The NEXAFS spectra were measured in the total electron yield (TEY) mode at an incident angle of 60°, and the light polarization was parallel to the surface (s-polarization) at any light incident angle; that is, there was no influence of the X-ray polarization. The intensity of the incident photon beam (I_0) was monitored at a gold mesh in front of the samples, enabling the TEY signal to be normalized by I_0. The total energy resolution was ~0.5 eV. The C *K*-edge NEXAFS spectra were measured in the energy range of 280 to 320 eV at an energy step of 0.1 eV. In this study, the absolute sp^2 content was evaluated from the π^* peak of C *K*-edge spectra, following the procedure given in the literatures [15–17].

The hydrogen content was measured via ERDA and RBS to support the results of NEXAFS, as described in more detail elsewhere [18, 26]. Both ERDA and RBS were performed using an electrostatic accelerator (NT-1700HS: Nisshin-High Voltage Co.) located at the Extreme Energy-Density Research Institute, Nagaoka University of Technology, Japan. The spectra of the samples were acquired by using a 2.5 MeV-He^+ ion beam impacting the sample surface at an incident angle of 72° with respect to the surface normal of the sample. For ERDA and RBS measurements, He^+ ions that collided with and were scattered elastically by the sample were detected with a solid-state detector (SSD) arranged at 78° and 12° of the ERDA and RBS, respectively, with respect to surface normal of samples toward and backward from the incident beam, respectively; these data pieces were used to obtain the hydrogen contents of the films.

3. Results and Discussion

3.1. Thickness and True Density Measurement of a-C:H Films by XRR. Figures 1(a)–1(d) show the XRR curves of the *a*-C:H films at various thicknesses. The black curves represent the experimental XRR profiles. For the simulation analysis, a two-layer model consisting of an *a*-C:H film and an interface

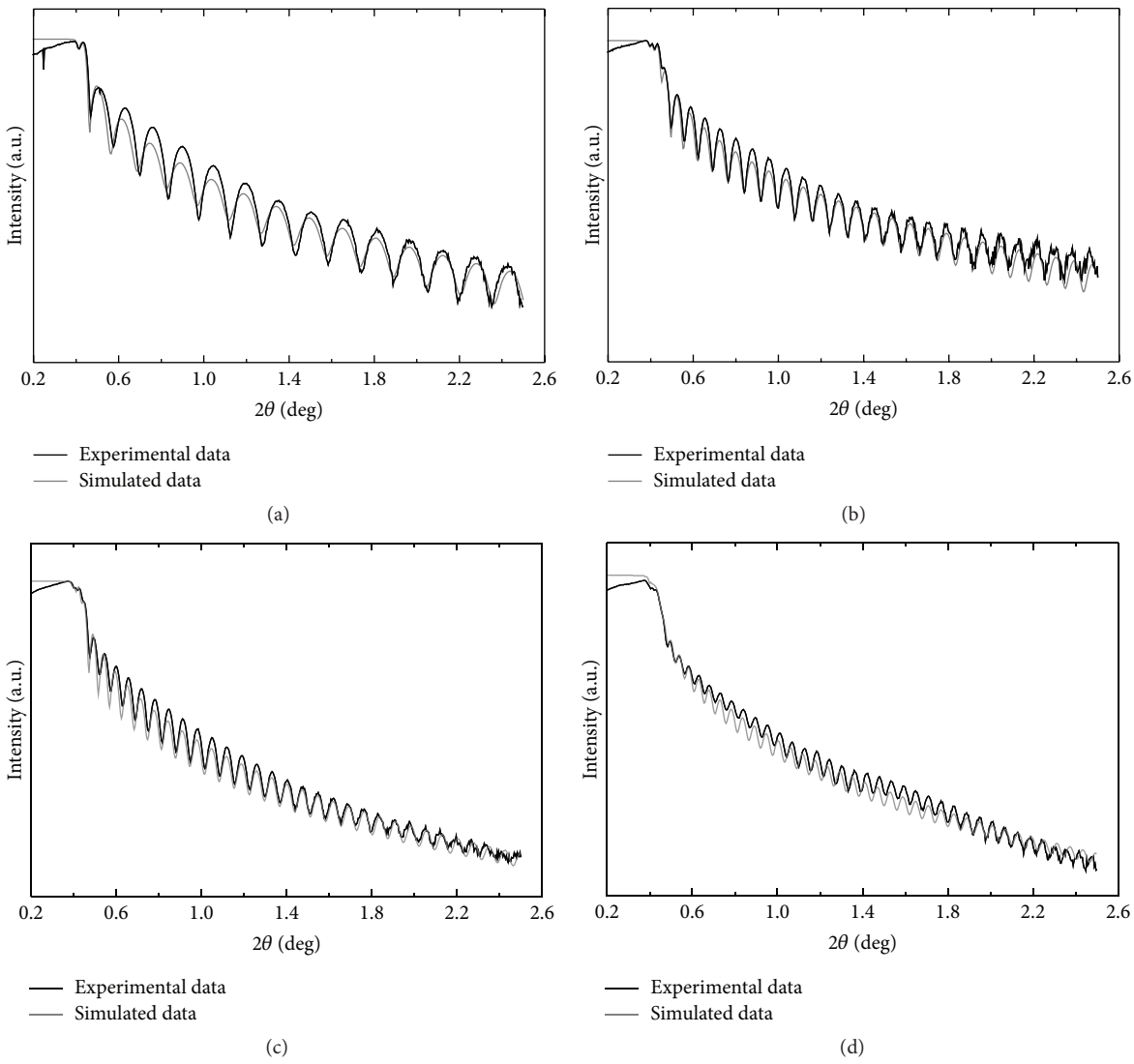

Figure 1: The XRR profiles of the *a*-C:H films deposited at various thicknesses: (a) 55 nm, (b) 101 nm, (c) 118 nm, and (d) 143 nm.

layer between the film and the Si substrate was used [27]. The gray curves in Figure 1 are the simulation profiles with the appropriate thickness and true density values of the films at the incident angle range of 0.2° to 2.6°.

The relationship between the thickness and true density of the *a*-C:H films as a function of the deposition time is shown in Figure 2. The evaluated film thicknesses from the XRR profiles of the A, B, C, and D samples were 55, 101, 118, and 143 nm, respectively. From these results, it can be interpreted that, with the increase of the deposition time, the film thickness increased with a deposition rate of ~15.8 nm/min. Generally, the deposition rate for the initial deposition is distinctively larger than that for a longer duration, while the latter becomes almost constant for a long deposition time, as discussed in [28]. Therefore, the deposition rate depends on several parameters, such as temperature and bias voltage [29]. Moreover, the true density measurement showed that the densities of films A, B, C, and D were 1.77, 1.75, 1.76, and 1.78 g/cm^3, respectively, which are almost independent of the film thickness. From this observation, it is not necessary to consider the true density in discussing the sp^2 content. Thus, the description in terms of the sp^2 content is directly related to the hydrogen content as a function of the film thickness.

3.2. sp^2 Content Measurement of a-C:H Films by NEXAFS. The C *K*-edge NEXAFS spectra of the *a*-C:H films at various thicknesses are shown in Figure 3. The spectra of all the *a*-C:H films were decomposed into the primary two-edge structures. The preedge resonance located at 284.6 eV is associated with C 1*s* $\rightarrow$ π^* (C=C) transition from sp^2 site, including the contribution of the π^* (C≡C) state. However, this peak is barely observed in the diamond spectra because diamond consists of only carbon atoms in sp^3 site [5]. The high energy-edge from 288.6 eV to 320.0 eV is related to C 1*s* $\rightarrow$ σ^* (C–C) transitions from *sp*, sp^2, and sp^3 hybridization, presenting a broad structure of amorphous carbon film due to the different superpositions of sp^2 and sp^3 arrangements and

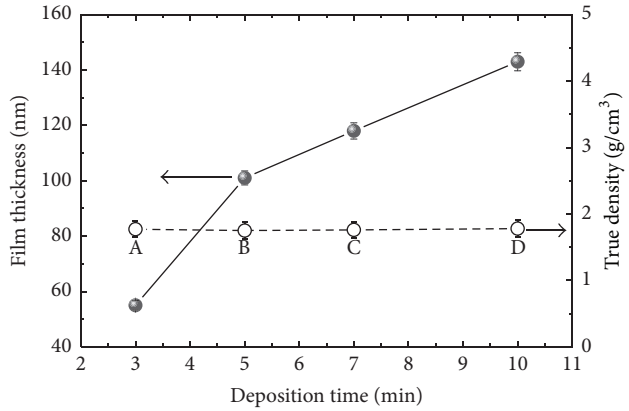

Figure 2: The relationship between the film thickness and the true density of the *a*-C:H films as a function of the deposition time.

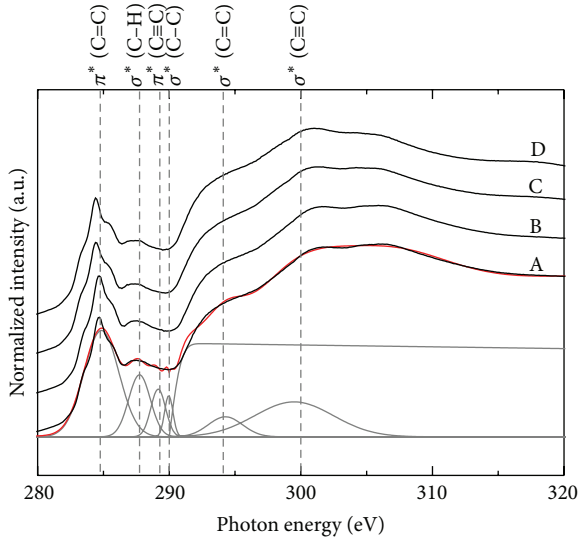

Figure 3: Carbon *K*-edge NEXAFS spectra of the *a*-C:H films grown via a RF-PECVD method at various thicknesses.

atomic intermixing [19, 30]. Surprisingly, the peak located at approximately 286.6 eV was found to be attributed to the σ^* (C–H) state, which indicates bonding between the carbon and hydrogen atoms in the local structure of the *a*-C:H films. Note that the intensity of such σ^* (C–H) peak is closely correlated with the hydrogen content evaluated from ERDA and RBS. However, there is an obvious σ^* (C–C) state located at approximately 288.8 eV that may be partially replaced by the σ^* (C–H) state via the hydrogenation process, leading to the suppression of the σ^* (C–C) state. In addition, some contributions from oxygen atoms might exist in the form of the π^* (C=O) and σ^* (C–O) states in the range of 286.0 to 290.0 eV and ~305.0 eV due to contamination from the environment [14, 20]. Note that the edge jump at around 290.0 eV (ionization potential) was fitted with an error-function step and the subtracted spectra are decomposed into Gaussian peaks [11, 16].

To clarify the features of the C *K*-edge NEXAFS spectra, the peak positions obtained in the present work are

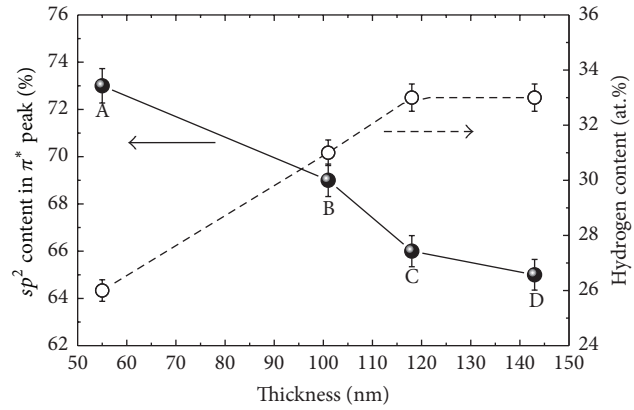

Figure 4: The sp^2 and hydrogen contents of the *a*-C:H film as a function of the film thickness.

compared with those in previous works [4, 10, 19, 20]; for this comparison, the peak positions of the *a*-C:H films are summarized in Table 1. Clearly, the peak positions are almost independent of the synthesis and growth conditions. Although we used the same method for growing the films as in the previous work [10], we successfully obtained all the main peak positions from the features of C *K*-edge NEXAFS spectra. In particular, the peaks of the π^* (C=C) and σ^* (C–H) states are explicitly observed in the spectra. Note that the features of amorphous carbon based materials from NEXAFS spectra can possess a near-surface region where the sp^2-hybridized state is promoted. However, note that the intensity of π^* peak is slightly lower as the thickness increases from 55 to 143 nm.

The isolated π^* peak appears in the C *K*-edge NEXAFS spectra, corresponding to the carbon sp^2 bonding state formed in the *a*-C:H films. The arrangement of the sp^2 site in the local structure specifies the electronic, corrosion, and optical properties, while the sp^3 site controls the mechanical properties as well as the structure of the film [1–3]. Thus, the absolute sp^2 content in the films must be extracted using a quantitative analysis method. The sp^2 content can be extracted by normalizing the region of the resonance corresponding to C $1s \rightarrow \pi^*$ transitions at 284.6 eV of the NEXAFS spectra. In practice, the integrations are performed separately in the regions of 280 eV to 286 eV and 291 eV to 320 eV for the π^* and σ^* peaks, respectively, to avoid the influence of the σ^* (C–H) state. As a result, Figure 4 clearly shows the absolute sp^2 content and the hydrogen content as functions of the film thickness. The sp^2 content gradually decreases as the film thickness increases. The estimated absolute sp^2 contents of A, B, C, and D are 73, 69, 66, and 65%, respectively, which displayed sp^2-rich (>60%) *a*-C:H films. The reduction of the sp^2 content may cause the change of the unique properties of the films, such as electronic and optical properties [1]. In contrast, the sp^3 content is considered to increase with the increase of the thickness; however, note from the results presented in Figure 2 that the hydrogen content and the film thickness should be appropriately controlled to obtain the high quality of films.

Table 1: Comparison of the peak positions of the C *K*-edge NEXAFS spectra of the *a*-C:H films obtained from previous works and from the present work.

Samples	Peak positions (eV)						Reference
	π^* (C=C)	σ^* (C–H)	π^* (C≡C)	σ^* (C–C)	σ^* (C=C)	σ^* (C≡C)	
Previous works							
a-C:H†	285.5	288.0	—	—	293.0	303.8	[4]
a-C:H††	285.0	~287.0	—	~288.0	—	—	[10]
a-C:H†††	285.5	287.0–288.0	—	293.0	—	—	[19]
a-C:H††††	284.7	286.3	287.2	288.2	292.6	303.8	[20]
Present work							
A, B, C, D	284.6	286.6	~287.5	~288.8	293.0	300.2	—

†Electron cyclotron resonance chemical vapor deposition (ECR-CVD) method, ††plasma-enhanced chemical vapor deposition (PECVD) method, †††dip deposited method, and ††††pulsed laser deposition (PLD) method.

It has been reported that *a*-C:H films deposited by a CVD method have the stable sp^2 structural arrangement near the edge of the surface. Hence, the dose of ions with high kinetic energy with increasing deposition time may break the sp^2 structure on the surface and subsequently replace it with the sp^3 structure [2]. The observed relationship between the sp^2 content and the film thickness indicates that it may be feasible to classify them into two groups. The first group, at approximately 73% sp^2 content, was designed for a film thickness of approximately 55 nm. The second group, with an sp^2 content between 65% and 69%, was designed for film thicknesses from 101 to 143 nm. From the above considerations, the film thickness may play an important role in the bonding formation of the chemical structure in amorphous carbon films when analyzing the NEXAFS data.

3.3. H Content Measurement of a-C:H Films by ERDA/RBS. Figures 5(a)–5(d) show the typical ERDA and RBS spectra that were simultaneously obtained for the *a*-C:H films. The peaks related to the hydrogen, carbon, and silicon atoms appear on the spectra. The H peaks on ERDA spectra derived from the *a*-C:H films were profiled using an ERDA fitting calculation package (Nissin High Voltage ERDA ver. 1.55) by comparing the peak intensities of H and C elements. The C and Si peaks on RBS spectra derived from the *a*-C:H films and substrates were profiled using the RBS fitting calculation package (Nissin High Voltage ERNIE ver. 1.0). The estimation error of fitting process was around 0.5 at.% for this study.

From the results of the ERDA and RBS spectra, the atomic fractions of hydrogen in A, B, C, and D are 26, 31, 33, and 33 at.%, respectively. These results demonstrated that the hydrogen content of the *a*-C:H films is 50–60% of that of the C_6H_6 source gas. Hence, the incorporation of source gas into the film structure may be negligible; therefore, the obtained amount of hydrogen content can confirm that the *a*-C:H film is the DLC film. The hydrogen atom must bond to the carbon atom and then form a C–H bond. From Figure 4, the hydrogen content increases with the increase of the film thickness. In addition, the stable hydrogen configuration within the carbon matrix reduced the degree of graphitization [4], which corresponded to a significant decrease of sp^2 content in the films in the NEXAFS measurement. However, in this work, the bias voltage was fixed at −0.4 kV; thus, the increment of the hydrogen is caused only by the increase of the thickness from 55 to 143 nm. It was suggested that the hydrogen content may be saturated at a longer deposition time.

Furthermore, it has been reported that the total gas pressure and negative bias voltage affected the hydrogen incorporation in the film [31–33]. From the ERDA and RBS results, it was confirmed that 2.5 MeV-He^+ irradiation promotes dehydrogenation of films without structural transfer from sp^3 to sp^2 hybridization [25]. However, these results suggest that the size of the clusters (a small cluster of the sp^2 site) in the films is limited by the hydrogen termination, and the cluster size can be decreased with the increase of the hydrogen content as a function of the film thickness.

4. Conclusions

The compositions and bonding states of *a*-C:H films were evaluated using NEXAFS and ERDA/RBS measurements. The sp^2 contents in the films were slightly decreased, whereas the hydrogen contents were increased with the increase of the film thickness from 55 to 143 nm. In addition, the features of C *K*-edge NEXAFS spectra distinctly exhibited the promotion of the transitions of the π^* (C=C), σ^* (C–H), σ^* (C=C), and σ^* (C≡C) states and the suppression of the transitions of the π^* (C≡C) and σ^* (C–C) states as the thickness increases. This investigation successfully evaluated the composition and bonding state in the *a*-C:H films at various thicknesses.

Conflict of Interests

The authors declare that there is no conflict of interests regarding the publication of this paper.

Acknowledgments

The authors are grateful to the Japanese Government (Ministry of Education, Culture, Sports, Science and Technology, MEXT) for granting the financial support and scholarships under Contract no. 133142. Additionally, the authors sincerely appreciate the assistance from the staff at 3.2a beamline in

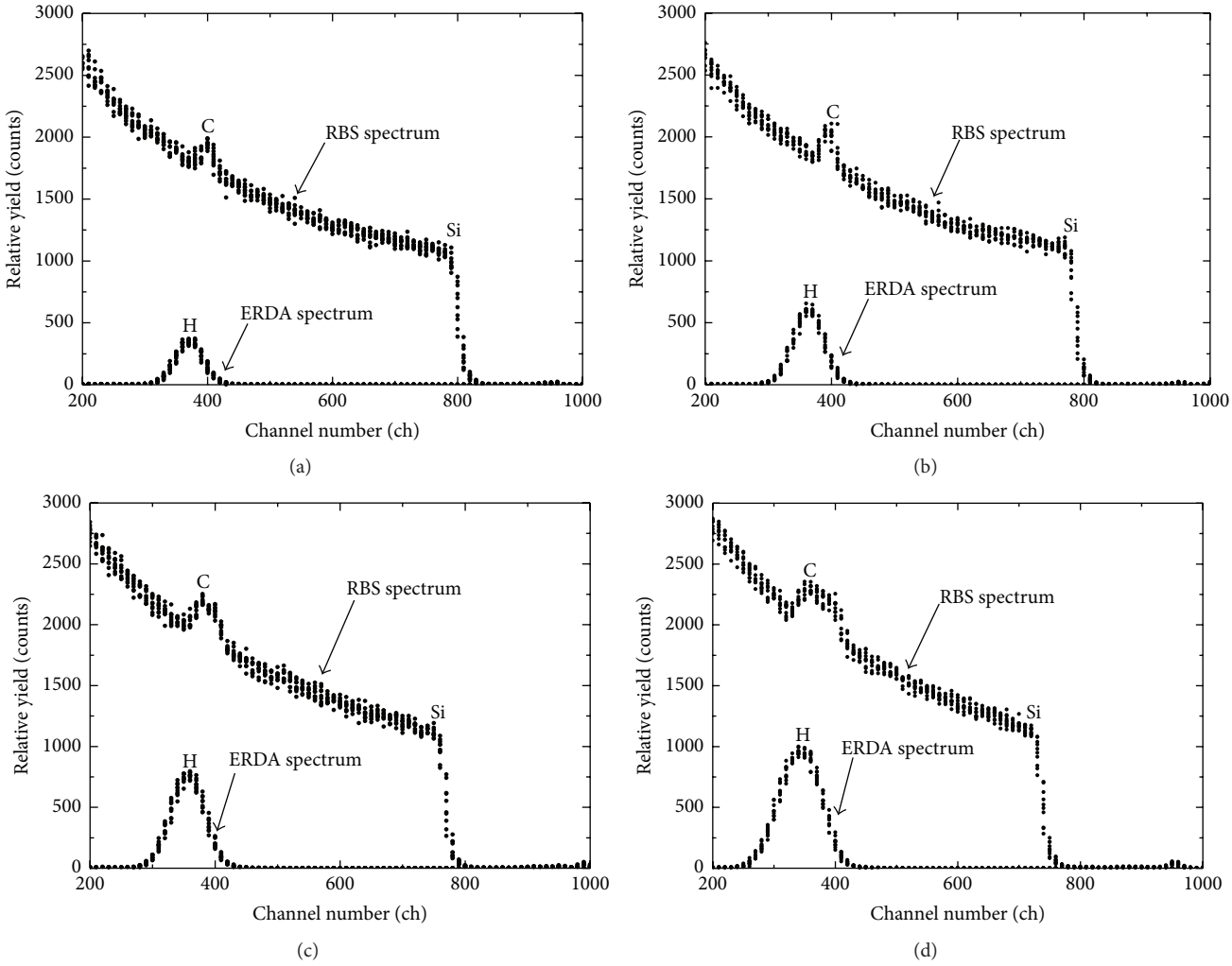

Figure 5: ERDA and RBS spectra of the *a*-C:H films prepared at various thicknesses: (a) 55 nm (A sample), (b) 101 nm (B sample), (c) 118 nm (C sample), and (d) 143 nm (D sample).

Synchrotron Light Research Institute (Public Organization), Thailand, for NEXAFS measurement.

References

[1] F. Piazza, D. Grambole, D. Schneider, C. Casiraghi, A. C. Ferrari, and J. Robertson, "Protective diamond-like carbon coatings for future optical storage disks," *Diamond and Related Materials*, vol. 14, no. 3–7, pp. 994–999, 2005.

[2] K. Bewilogua and D. Hofmann, "History of diamond-like carbon films—from first experiments to worldwide applications," *Surface and Coatings Technology*, vol. 242, pp. 214–225, 2014.

[3] J. C. Damasceno, S. S. Camargo Jr., and M. Cremona, "Optical and mechanical properties of DLC-Si coatings on polycarbonate," *Thin Solid Films*, vol. 433, no. 1-2, pp. 199–204, 2003.

[4] J. G. Buijnsters, R. Gago, A. Redondo-Cubero, and I. Jiménez, "Hydrogen stability in hydrogenated amorphous carbon films with polymer-like and diamond-like structure," *Journal of Applied Physics*, vol. 112, no. 9, Article ID 093502, 2012.

[5] T. Kitagawa, K. Miyauchi, K. Kanda et al., "Near edge X-ray absorption fine structure study for optimization of hard diamond-like carbon film formation with Ar cluster ion beam," *Japanese Journal of Applied Physics*, vol. 42, no. 6, pp. 3971–3975, 2003.

[6] A. Saikubo, N. Yamada, K. Kanda et al., "Comprehensive classification of DLC films formed by various methods using NEXAFS measurement," *Diamond and Related Materials*, vol. 17, no. 7–10, pp. 1743–1745, 2008.

[7] K. Kanda, T. Kitagawa, Y. Shimizugawa et al., "Characterization of hard diamond-like carbon films formed by Ar gas cluster ion beam-assisted fullerene deposition," *Japanese Journal of Applied Physics*, vol. 41, pp. 4295–4298, 2002.

[8] K. Kanda, Y. Shimizugawa, Y. Haruyama et al., "NEXAFS study on substrate temperature dependence of DLC films formed by Ar cluster ion beam assisted deposition," *Nuclear Instruments and Methods in Physics Research Section B: Beam Interactions with Materials and Atoms*, vol. 206, pp. 880–883, 2003.

[9] G. Hähner, "Near edge X-ray absorption fine structure spectroscopy as a tool to probe electronic and structural properties of thin organic films and liquids," *Chemical Society Reviews*, vol. 35, no. 12, pp. 1244–1255, 2006.

[10] F. Mangolini, J. B. McClimon, F. Rose, and R. W. Carpick, "Accounting for nanometer-thick adventitious carbon contamination in X-ray absorption spectra of carbon–based materials," *Analytical Chemistry*, vol. 86, no. 24, pp. 12258–12265, 2014.

[11] J. Stöhr, *NEXAFS Spectroscopy*, Springer, New York, NY, USA, 1992.

[12] J. Díaz, S. Anders, X. Zhou, E. J. Moler, S. A. Kellar, and Z. Hussain, "Analysis of the π^* and σ^* bands of the x-ray absorption spectrum of amorphous carbon," *Physical Review B*, vol. 64, no. 12, Article ID 125204, 19 pages, 2001.

[13] J. Diaz, O. R. Monteiro, and Z. Hussain, "Structure of amorphous carbon from near-edge and extended x-ray absorption spectroscopy," *Physical Review B: Condensed Matter and Materials Physics*, vol. 76, no. 9, Article ID 094201, 2007.

[14] C. Lenardi, P. Piseri, V. Briois, C. E. Bottani, A. Li Bassi, and P. Milani, "Near-edge X-ray absorption fine structure and Raman characterization of amorphous and nanostructured carbon films," *Journal of Applied Physics*, vol. 85, no. 10, pp. 7159–7167, 1999.

[15] F. L. Coffman, R. Cao, P. A. Pianetta, S. Kapoor, M. Kelly, and L. J. Terminello, "Near-edge x-ray absorption of carbon materials for determining bond hybridization in mixed sp^2/sp^3 bonded materials," *Applied Physics Letters*, vol. 69, article 568, 1996.

[16] D. A. Outka and J. Stöhr, "Curve fitting analysis of near-edge core excitation spectra of free, adsorbed, and polymeric molecules," *The Journal of Chemical Physics*, vol. 88, no. 6, pp. 3539–3554, 1988.

[17] A. V. Sumant, P. U. P. A. Gilbert, D. S. Grierson et al., "Surface composition, bonding, and morphology in the nucleation and growth of ultra-thin, high quality nanocrystalline diamond films," *Diamond and Related Materials*, vol. 16, no. 4–7, pp. 718–724, 2007.

[18] Y. Ohkawara, S. Ohshio, T. Suzuki, H. Ito, K. Yatsui, and H. Saitoh, "Quantitative analysis of hydrogen in amorphous films of hydrogenated carbon nitride," *Japanese Journal of Applied Physics*, vol. 40, no. 12, pp. 7007–7012, 2001.

[19] S. C. Ray, H. M. Tsai, J. W. Chiou et al., "X-ray absorption spectroscopy (XAS) study of dip deposited a-C:H(OH) thin films," *Journal of Physics: Condensed Matter*, vol. 16, no. 32, pp. 5713–5719, 2004.

[20] T. Yoshitake, S. Ohmagari, A. Nagano et al., "Near-edge X-ray absorption fine structure of ultrananocrystalline diamond/hydrogenated amorphous carbon films prepared by pulsed laser deposition," *Journal of Nanomaterials*, vol. 2009, Article ID 876561, 5 pages, 2009.

[21] C. B. Fischer, M. Rohrbeck, S. Wehner, M. Richter, and D. Schmeißer, "Interlayer formation of diamond-like carbon coatings on industrial polyethylene: thickness dependent surface characterization by SEM, AFM and NEXAFS," *Applied Surface Science*, vol. 271, pp. 381–389, 2013.

[22] A. Catena, T. McJunkin, S. Agnello, F. M. Gelardi, S. Wehner, and C. B. Fischer, "Surface morphology and grain analysis of successively industrially grown amorphous hydrogenated carbon films (*a*-C:H) on silicon," *Applied Surface Science*, vol. 347, pp. 657–667, 2015.

[23] L. G. Parratt, "Surface studies of solids by total reflection of x-rays," *Physical Review*, vol. 95, no. 2, pp. 359–369, 1954.

[24] H. Nakajima, A. Tong-on, N. Sumano et al., "Photoemission spectroscopy and photoemission electron microscopy beamline at the Siam Photon Laboratory," *Journal of Physics: Conference Series*, vol. 425, no. 13, Article ID 132020, 2013.

[25] P. Songsiriritthigul, B. Kjornrattanawanich, A. Tong-on, and H. Nakajima, "Design of the first undulator beamline for the Siam Photon Laboratory," *Nuclear Instruments and Methods in Physics Research Section A*, vol. 582, no. 1, pp. 100–102, 2007.

[26] Y. Ohkawara, S. Ohshio, T. Suzuki, H. Ito, K. Yatsui, and H. Saitoh, "Dehydrogenation of nitrogen-containing carbon films by high-energy He^{2+} irradiation," *Japanese Journal of Applied Physics*, vol. 40, no. 5, pp. 3359–3363, 2001.

[27] M. F. Toney and S. Brennan, "Measurements of carbon thin films using x-ray reflectivity," *Journal of Applied Physics*, vol. 66, no. 4, pp. 1861–1863, 1989.

[28] T. Harigai, Y. Yasuoka, N. Nitta, H. Furuta, and A. Hatta, "X-ray reflectivity analysis on initial stage of diamond-like carbon film deposition on Si substrate by RF plasma CVD and on removal of the sub-surface layer by oxygen plasma etching," *Diamond and Related Materials*, vol. 38, pp. 36–40, 2013.

[29] N. Paik, "High-density DLC films prepared using a magnetron sputter type negative ion source," *Diamond and Related Materials*, vol. 14, no. 2, pp. 196–200, 2005.

[30] I. Jiménez, R. Gago, and J. M. Albella, "Fine structure at the X-ray absorption π^* and σ^* bands of amorphous carbon," *Diamond and Related Materials*, vol. 12, no. 2, pp. 110–115, 2003.

[31] K. Ozeki, D. Sekiba, A. Uedono, K. Hirakuri, and T. Masuzawa, "Effect of incorporation of deuterium on vacancy-type defects of a-C:H films prepared by plasma CVD," *Applied Surface Science*, vol. 330, pp. 142–147, 2015.

[32] M. A. Tamor and W. C. Vassell, "Raman 'fingerprinting' of amorphous carbon films," *Journal of Applied Physics*, vol. 76, no. 6, pp. 3823–3830, 1994.

[33] K. Ozeki, I. Nagashima, Y. Ohgoe, K. K. Hirakuri, H. Mukaibayashi, and T. Masuzawa, "Gas barrier properties of diamond-like carbon films coated on PTFE," *Applied Surface Science*, vol. 255, no. 16, pp. 7286–7290, 2009.